Vortex-Concept for Radioactivity Release Prevention at NPP: Development of Computational Model of Lab-Scale Experimental Setup

Sana Ullah [a*], Yim, Man Sung [a], [b]Jinsoo Park, [b]Hyung Jin Sung
[a]*Department of Nuclear and Quantum Engineering (NQe),* [b]Department of Mechanical Engineering,
Korea Advanced Institute of Science and Technology (KAIST), Daejoen, 34141, Republic of Korea.
[*]*Corresponding author: msyim@kaist.ac.kr*

1. Introduction

In the event of a severe accident, the airborne radionuclides will accumulate inside reactor containment, the last barrier. On containment failure, this radioactive material will escape to the environment, posing serious threat to public health and environmental safety. To prevent dispersion of this leaking radioactive material to environment, an innovative safety system based on vortex-like air curtain was proposed. It was hypnotized that an air curtain, generated by a number of blowing towers, positioned around the damaged containment building could contain and collect leaking radioactive material for treatment. The preliminary investigations of various system configurations were previously performed using CFD approach, and an optimized configuration was proposed [1].

The experimental validation of the vortex-like air curtain concept and use of an appropriate CFD modelling approach for analyzing the problem becomes crucial. A lab-scale experimental setup is designed to validate the proposed concept and CFD modeling approach as a part of validation process. In this study, a computational model of this lab-scale experiment setup is developed using open source CFD code OpenFOAM. The computational results will be compared with experimental data for validation purposes in future, when experimental data is available.

2. Experimental setup

An experimental setup is developed to validate the concept of artificial vortex-like airflow generation around reactor containment. A scale-down model of a typical PWR containment with a diameter of 150 mm and a height of 276 mm is placed inside a closed rectangular chamber, 800mm wide/long and 1050mm high. Airflow generation is through the use of four (4) towers, symmetrically located at chamber diagonals. There are eight (8) nozzles per tower, each equipped with flow control valve to control nozzle flow. The air will be supplied by the campus compress-air facility. The nozzle angle and distance from the model is adjustable. The bottom four (4) nozzles are sufficient to cover model completely, therefore it is decided to use bottom four (4) nozzles for conducting all the experiments.

The particle image velocimetry (PIV) setup was used for collecting experiment data. The PIV setup consists of a laser, a pulse/delay generator, a beam expander, and a high-speed camera. The laser light is produced by a 532-nm Nd:YAG double-pulse laser (Solo 200XT, NEW WAVE). The double-pulse laser is operated at 15 Hz with an energy of approximately 150 mJ/pulse. It is expanded to form a light sheet with a thickness of 1.5 mm using a cylindrical Galilean beam expander. The beam expander is composed of a Plano-Convex and a Plano-Concave cylindrical lens.

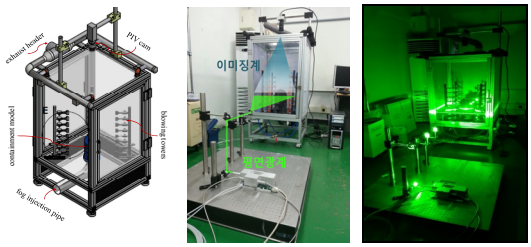

Fig. 1. Experimental setup

The light sheet is positioned at a height of 120 mm from the model base. However, due to PIV measurement limitations, only a portion of flow field (Fig. 2) can be measured. A fog generator (HZ-400, Antari) was used to generate seeding particles for PIV image acquisition.

Table 1: Experimental setup specifications

Chamber size	(800×800×1050) $(mm)^3$	
Containment	diameter: 150mm	height: 276mm
Towers	No. : 4	Height: 310mm
Nozzles	No. per tower: 4	length: 41mm
	Width: 6mm	
PIV setup for flow field measurement	plane: 120mm	
	grid : 11×19	
	region: x (mm): ±80	y (mm): -120:-40

Fog particles were illuminated by the planar light sheet, and the 8-bit grayscale particle images were captured using a high-speed camera (PCO 1200hs, PCO) with a resolution of 1,280x1,024 pixels. The image acquisition using the high-speed camera is synchronized with the double-pulse laser using a pulse/delay generator (BNC model 565). The inter-frame time of successive laser pulses was set to be 2 ms by the pulse/delay generator.

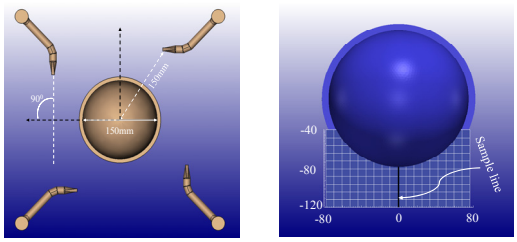

Fig. 2. Important model dimensions and PIV measurement grid.

3. Development of computational model

The computational model of experimental setup was prepared in OpenFOAM. The OpenFOAM framework is based on the finite volume approach, and consists of C++ libraries, used primarily to create executable (i.e. applications). The applications are either solvers or utilities. Each solver is designed to solve a specific problem, while utilities are for data manipulations [2].

3.1. Governing equations

The model was based on steady state incompressible RANS (Reynolds Averaged Navier-Stokes) equations of fluid dynamic. The one-equation eddy-viscosity Spalart Allmaras (SA) [3] model was used for the closure of RANS system of equations.

3.2. Preparation of geometry and mesh

The computational domain was prepared as per the chamber size. Only four bottom nozzles per tower were modelled instead of eight for reducing unnecessary computational efforts. The OpenFOAM native meshing tool *SnappyHexMesh* was used to generate mesh. Mesh independence study was performed for base experimental setup presented in Fig. 3.

3.3. Boundary conditions

In current experiment setup, exhaust was provided at the top through four 42mm diameter pipe holes managed by a simple on/off exhaust fan connected to a common header pipe (referred to Fig.1 (a)). This exhaust setup could be tricky to flow stability inside chamber, because any imbalance between flow drawn out by the exhaust and flow thrown in by nozzles could induce instability inside the chamber. In fact, this proved to be the case, when analyzed (see discussion in section 4.2). Therefore, this forced to analyze other options for a better outlet conditions for experimentation. One simple choice was to leave top of the chamber open, and let flow establish inside the chamber. This condition proved sufficient for a stable flow inside the chamber.

For chamber sidewalls, three (3) different boundary conditions were investigated to gain advantage in the form of computational time, and accuracy, if any.

(a) Slip walls
(b) No-slip (wall resolution)
(c) No-slip (wall function)

The containment, tower and chamber ground were implemented as no-slip in all three cases. The scalable Spalding's law wall function was utilized for no-slip (wall function) treatment. The nozzles had fixed values at the given velocity.

3.4. Discretization schemes and solvers

The use of a particular discretization scheme may affect the accuracy and stability of solution. The first order schemes provide better stability but are less accurate as compared to the second order or blended (first-second order) schemes. Therefore, for exploring right choice of discretization schemes for present model, following two set of discretization schemes were compared:

(1) First order *upwind* scheme for divergence of all variables.
(2) First-second order blended *linearUpwindV,* and second order *limitedLinear1* schemes for divergence of velocity and modified turbulent viscosity respectively.

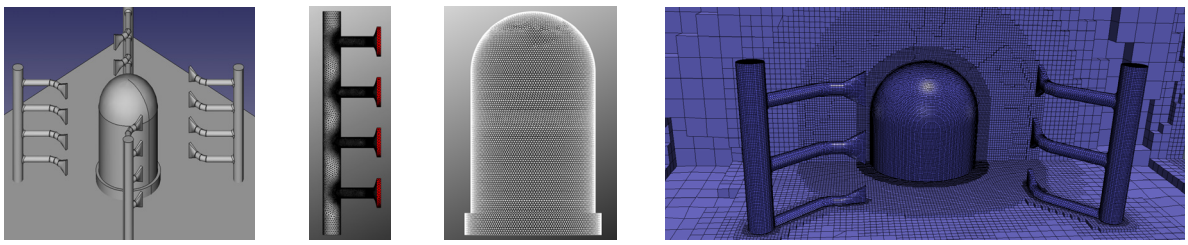

Fig. 3. The CAD model, corresponding surface mesh, and volume mesh for computation modelling of experimental setup.

The second order accurate *linear* discretization was used for estimating gradient terms. The well-known steady state solver semi-implicit pressure linked equations (SIMPLE) algorithm, implemented as simpleFoam in OpenFOAM was used.

4. Results and Discussion

The PIV was setup to provide data on XY plan at z=120mm. However, due to PIV limitations, the measurements would be available for the region shown in Fig. 2. To be consistent with experimental measurements, results of current CFD model were analyzed for the same region. For comparing the effect of various CFD parameters on the flow field, data were sampled along the line indicated in Fig. 2.

4.1. Mesh sensitivity analysis

For mesh sensitivity analysis, four different mesh resolutions were used. The cell count in each next refinement was at least 1.5 times the cell count in the previous refinement. The velocity data plots along the sample line are shown in Fig.4. This comparison showed that sufficient mesh independence was achieved at 1.5m cells with the current refinement strategy. To be conservative, it was concluded that a mesh having cell count of the order of 2.0m would be used for all the current and future analysis.

Table 2: Statistics for mesh sensitivity analysis

Parameters	M-1	M-2	M-3	M-4
No. of cells (millions)	1.0	1.5	2.34	3.9

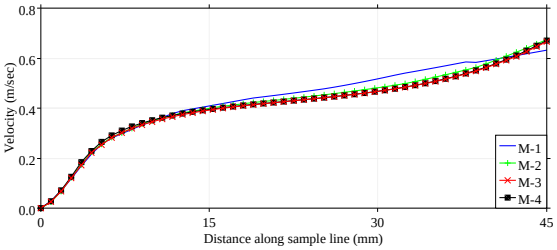

Fig. 4. Comparison of velocity profiles along sample line for mesh independence study.

4.2. Boundary conditions

As discussed earlier, chamber exhaust was provided at the top wall via four 42mm diameter holes driven by an exhaust fan. Modelling of the experimental setup with this configuration, failed to provide any stable solution whatsoever because of growing continuity imbalance. It is worth mentioning that both steady state and transient cases with various possible boundary conditions were investigated for reaching this conclusion. As a result, it was recommended to modify experimental setup, i.e., opening at least one side of the chamber, preferably the top for establishment of stable flow inside the chamber. The model with open top produced stable and physically correct results with negligible continuity imbalance. Consequently, all the results produced in this work, were modelled with open top.

With the chamber top serving as outlet boundary, further analysis with various boundary conditions for chamber walls, and other surfaces discussed in section 3.3, were performed. The results showed that, flow field within the region of interest was largely independent of the choice of boundary conditions at the chamber walls. However, saving of one hour of computation time was observed with the no slip boundary over the slip boundary for 5000 iteration. Therefore, the no slip boundary condition at chamber walls was recommended.

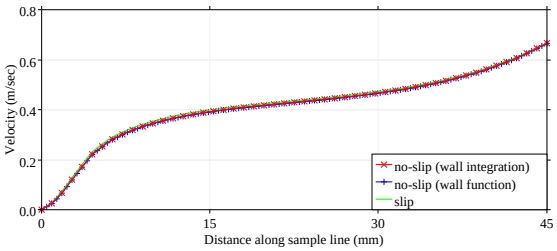

Fig. 5. Comparison of velocity profiles along sample line different types of boundary conditions

4.3. Discretization scheme

The first order discretization schemes are usually associated with numerical diffusion, which was evident from the current analysis as well: The first order schemes resulted in similar velocity profile with higher magnitude across the flow direction in comparison to the second order schemes. Furthermore, no issues of unboundedness and convergence were observed for the current setup. Therefore, use of second order schemes were recommended for computational modeling of the current experimental setup.

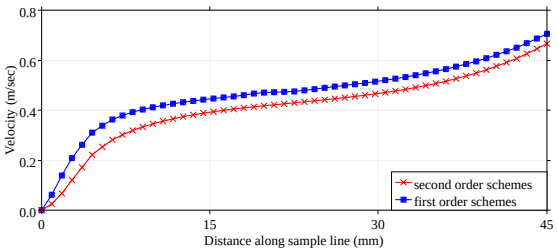

Fig. 6. Comparison of velocity profiles along sample line for first and first-second order blended discretization schemes.

4.4. Final CFD parameters for computational modelling of experimental setup

Final CFD parameters for numerical simulation of experimental setup are summarized in Table-3. These parameters were used to predict flow field inside the chamber (Fig. 6). The vector field and flow streamlines exhibited a flow, covering the containment model under simulated conditions.

Table 3: Final CFD parameters for computational model of experimental setup

Analysis type	Steady state RANS with SA turbulence model
Solver	simpleFoam
Mesh size	~2 million
Boundary conditions	walls: no-slip (wall resolution) outlet: top wall
Discretization schemes	Div. (V): linearUpwindV Div. (nuTilda): limitedLinear 1 Grad.: linear

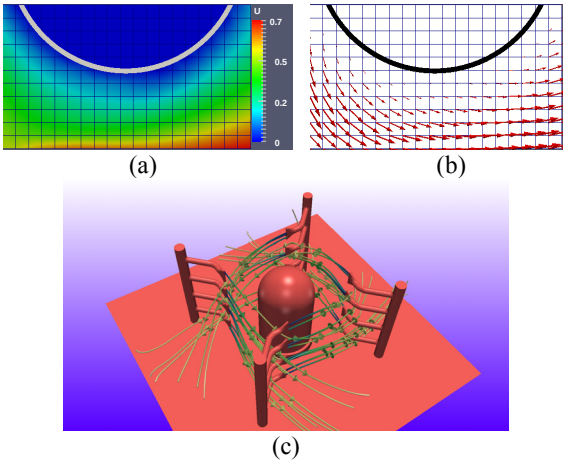

Fig. 7. (a) Velocity magnitude, (b) vector field, and (c) flow streamlines predicted by CFD model.

This model will further be validated for the lab-scale experimental setup by comparing experimental and computational results for varying blowing speed, angle and distance from the model. Once validated, this model will be extended to study the design and implementation of the proposed concept to actual nuclear power plant conditions.

3. Conclusions

1) A computation model of a lab-scale experimental setup, designed to validate the concept of artificial vortex-like airflow generation for application to radioactivity dispersion prevention in the event of severe accident, was developed.
2) The mesh sensitivity study was performed and a mesh of about 2 million cells was found to be sufficient for this setup.
3) The current exhaust configuration proved unstable for any valid experimentation, therefore, opening of one side of the chamber preferably top was recommended.
4) The flow within the region of interest was virtually independent of the choice of boundary condition at chamber walls, and surfaces.

ACKNOWLEDGMENTS

This work is supported by the Nuclear Power Core Technology Development of the Korea Institute of Energy Technology Evaluation and Planning (KETEP) under the Ministry of Trade, Industry & Energy, Republic of Korea (No. 20131510400050).

REFERENCES

[1] Sana Ullah et.al., “Preliminary Investigations of Vortex Based Ex-Containment Safety System for Severe Accident Management at NPPs”, ICAPP 2016, San Francisco, USA
[2] OpenFOAM, “User's Guide (2.3.0/3.0.0)”, OpenCFD, London, (2014). (http://www.openfoam.com)
[3] Spalart, P. R. and Allmaras, S. R., "A One-Equation Turbulence Model for Aerodynamic Flows," Recherche Aerospatiale, No. 1 (1994).
[4] P R. Spalart and C L. Rumsey. "Effective Inflow Conditions for Turbulence Models in Aerodynamic Calculations", AIAA Journal, 45, No. 10 (2007).